Segregation of molecules at cell division reveals native protein localization

Dirk Landgraf, Burak Okumus, Peter Chien, Tania A. Baker & Johan Paulsson

Supplementary figures, tables, note, methods and videos:

Supplementary Figure 1	No spectral bleedthrough from the ClpP-Venus YFP or ClpP-sfGFP foci into the RFP channel.
Supplementary Figure 2	Degradation rates were measured in daughter cells after cell division. ClpP-FP foci generate post-division cell-to-cell variability.
Supplementary Figure 3	Western blot analysis shows that the ClpP-FP levels vary for different tags.
Supplementary Figure 4	Time-series showing micro-colony growth of *E. coli* cells harboring the ClpP-mGFPmut3 fusions and quantification of GFP levels.
Supplementary Figure 5	Venus YFP or superfolder GFP (sfGFP) do not form foci or aggregates in *E. coli* when expressed alone.
Supplementary Figure 6	mGFPmut3 fused to five apparently foci-forming proteins resulted in no or less foci formation than previously reported in FP libraries.
Supplementary Figure 7	Western blot analysis confirms that the FP tag is not cleaved off from the ClpP-FP and ClpX-FP fusion proteins.
Supplementary Figure 8	Western blot analysis shows that the SNAP tag is not cleaved off the fusion protein.
Supplementary Figure 9	*E. coli* cells are segmented based on an out-of-focus high-resolution phase image.
Supplementary Figure 10	ClpP-Dronpa molecules are uniformly distributed inside *E. coli* cells.
Supplementary Figure 11	ClpP-sfGFP foci still form and create post-division cell-to-cell variability at 30 ˚C.
Supplementary Table 1	Fluorescent proteins used in this study with their corresponding amino acid sequences.
Supplementary Table 2	Summarized localization data of the five reportedly foci-forming *E. coli* proteins.
Supplementary Table 3	*E. coli* strains used in this study.
Supplementary Table 4	Plasmids used in this study.

Supplementary Table 5	Primers used in this study.
Supplementary Note 1	Description of Supplementary Videos 1–8.
Supplementary Note2	Strain and plasmid constructions.
Supplementary Methods 1	Description of Western blot analysis.
Supplementary Video 1	Micro-colony growth of *E. coli* cells with ClpP-Venus YFP foci.
Supplementary Video 2	Degradation of mCherry-ssrA in the ClpP-Venus YFP strain shows that the foci generate post-division cell-to-cell variability.
Supplementary Video 3	Degradation of mCherry-ssrA in the wildtype strain displays very low cell-to-cell variability after cell division.
Supplementary Video 4	Live-cell HILO imaging of ClpA-mGFPmut3 strain.
Supplementary Video 5	Live-cell HILO imaging of ClpP-mGFPmut3 strain.
Supplementary Video 6	Live-cell HILO imaging of ClpX-mGFPmut3 strain.
Supplementary Video 7	Live-cell HILO imaging of mGFPmut3 alone expressed from the P_{clpX} promoter at the endogenous locus.
Supplementary Video 8	Micro-colony growth of *E. coli* cells with Hfq-mGFPmut3, PepP-mGFPmut3, IbpA-mGFPmut3, MviM-mGFPmut3 and FruK-mGFPmut3 fusions.

Note: Supplementary Videos 1–8 are available on the Nature Methods website.

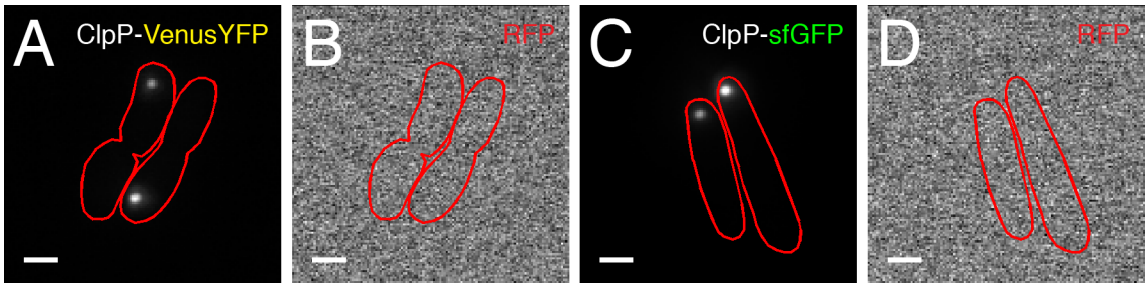

Supplementary Figure 1. The ClpP-Venus YFP and ClpP-sfGFP foci are not detected in the RFP channel. *E. coli* cells harboring the ClpP-Venus YFP (DHL436) or ClpP-sfGFP (DHL778) fusion were grown to exponential phase at 37 ˚C and imaged on an agar pad. YFP and GFP z-stacks (11 planes with 0.2 µm spacing between planes) were taken to visualize the ClpP-FP foci. Maximum projections of the z-stacks are shown (**A**: ClpP-Venus YFP and **C**: ClpP-sfGFP). These cells do not contain the mCherry-ssrA construct though RFP images (**B**: ClpP-Venus YFP and **D**: ClpP-sfGFP) with 200 ms exposure time (identical to the time-lapse imaging) were taken to confirm that the foci that can be seen in the RFP time-lapse movies (see **Supplementary Video 2**) are not due to spectral bleedthrough from the YFP or GFP into the RFP channel. mCherry-ssrA foci were not observed in the wildtype control experiment (DHL440, **Supplementary Video 3**) and are most likely caused by the artifactual ClpP-FP foci. This supports that the foci in the RFP image, seen in the time-lapse experiment, correspond to mCherry-ssrA molecules, which co-localize with the ClpP-FP foci. We observed that a small fraction of mCherry-ssrA molecules is not degraded in the time-lapse experiment (data not shown). We hypothesize that these immortal mCherry-ssrA molecules are due to translation errors in the *ssrA* tag or loss of the degradation tag although further investigation is needed to clarify this. Images are auto-scaled for display. The scale bar (white) corresponds to 1 µm. The red outline shows the cell boundary.

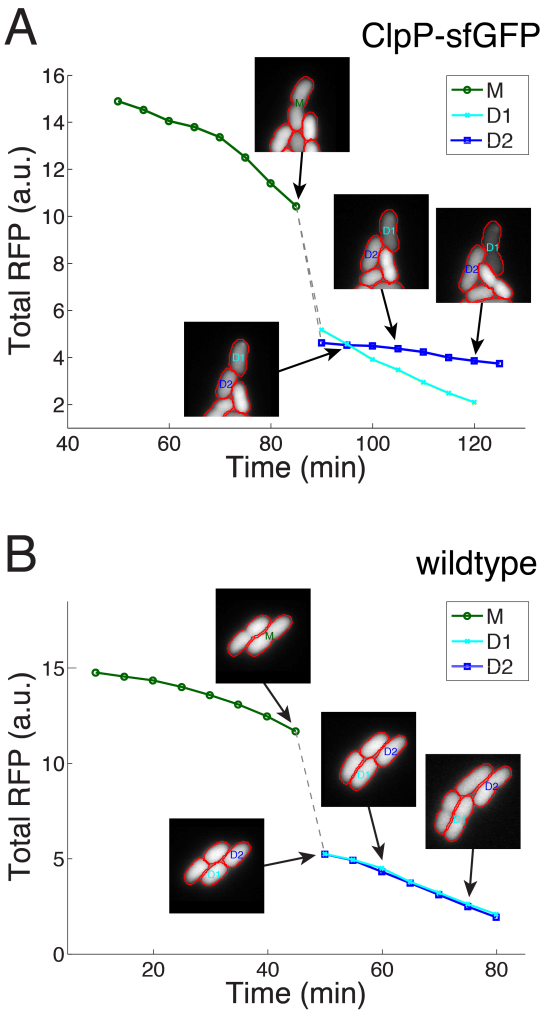

Supplementary Figure 2. ClpP-FP foci generate post-division cell-to-cell variability. (**A**) A mother cell (M, green) with a ClpP-sfGFP foci (strain DHL955) divides and daughter cell 1 (D1, cyan) inherits the ClpP-sfGFP focus (GFP images are not shown) and degrades an mCherry-ssrA reporter substrate much faster than daughter cell 2 (D2, blue). RFP images (insets) are shown for selected time-points (indicated by arrows). Cell outlines are shown in red. The degradation rate ratio (defined as degradation rate of the daughter with the faster rate divided by the daughter with the slower rate) is 4.02 here. (**B**) In strong contrast, very little post-division cell-to-cell variability was observed for the wildtype strain (DHL440). Both daughter cells (D1 and D2) have a very similar degradation rate after cell division. The degradation rate ratio is 1.04 for this sibling pair of the wildtype strain. The respective time-lapse movies were recorded at 30 ˚C (results are similar at 37 ˚C). The mCherry-ssrA degradation reporter is degraded in single cells with zeroth-order kinetics, as previously shown for GFP-ssrA[20]. The deviation of the RFP curve from a straight line at the beginning of the time-lapse experiment is because of delayed mCherry maturation and competition of non-matured mCherry molecules for degradation.

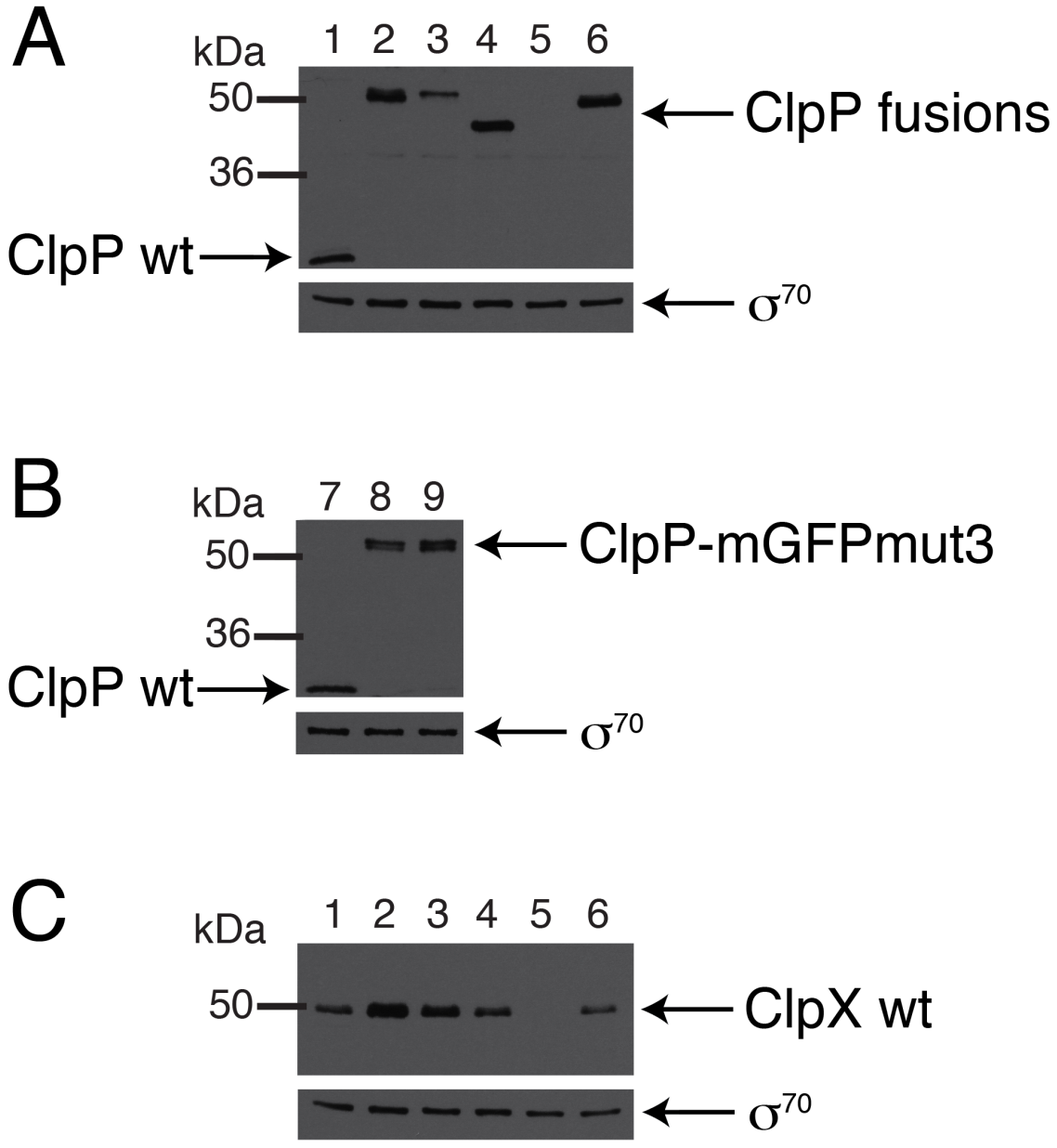

Supplementary Figure 3. Western blot analysis **(Supplementary Methods 1)** shows that the ClpP-FP levels vary for different tags. (**A**) The levels of the ClpP-Venus YFP (lane 2: DHL436), ClpP-SNAP tag (lane 4: DHL663) and ClpP-sfGFP (lane 6: DHL778) fusions are higher than the wildtype (lane 1: MC4100) whereas the ClpP-mGFPmut3 (lane 3: DHL661) fusion is lower than the wildtype (wt). Samples were prepared from exponential-phase cells grown at 37 ˚C and probed with the anti-ClpP antibody. The level of the ClpP-mGFPmut3 fusion is reduced, probably because mGFPmut3 lacks the F64L mutation, which increases the folding efficiency at 37 ˚C[21]. (**B**) The ClpP-mGFPmut3 level (lane 8: DHL661) is similar to the wildtype (lane 7: MC4100) at 30 ˚C and hence the segregation assay was performed at 30 ˚C for ClpP-mGFPmut3 (**Fig 3**, lower row). A strain expressing two copies of ClpP-mGFPmut3 has higher ClpP levels (lane 9: DHL986) than the wildtype at 30 ˚C (lane 7), and the average GFP fluorescence per cell is ~2.0× as high as for the strain with one copy of ClpP-mGFPmut3 (**Supplementary Fig. 4**). The ClpP-mGFPmut3 band doublet (lane 8 and 9) corresponds probably to ClpP-mGFPmut3 with and without the 14 amino acid leader sequence[22]. (**C**) The ClpX abundance is also affected by the various FP tags to ClpP probably due to polarity effects. Western blot samples were prepared from exponential-phase cells grown at 37 ˚C and probed with the anti-ClpX antibody. The anti-ClpP and

anti-ClpX antibodies are specific for their respective antigens, as confirmed with the Δ*clpPX* deletion strain (lanes 5: DHL708). σ^{70} (also known as RpoD) levels were measured and used as a loading control.

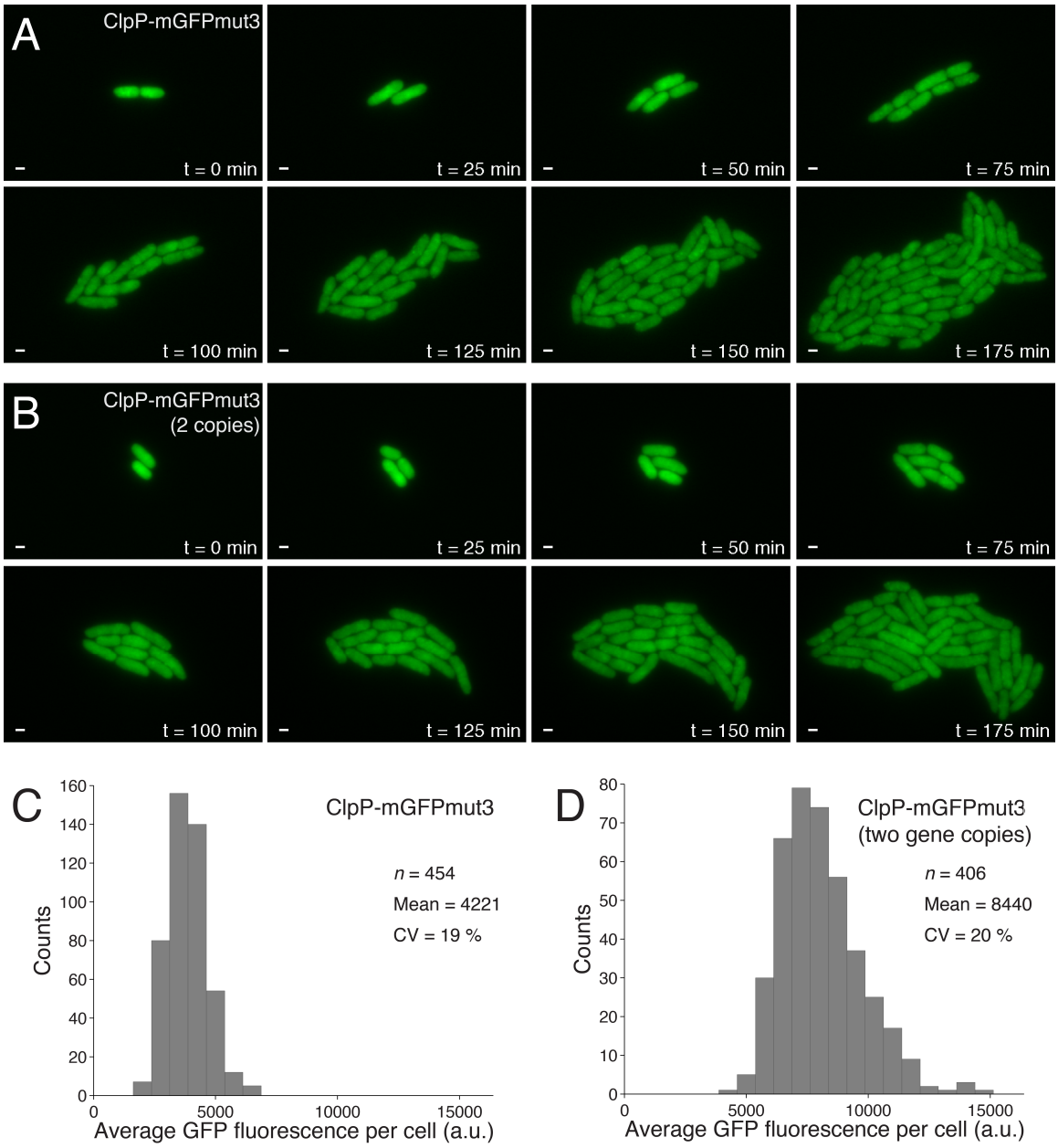

Supplementary Figure 4. Micro-colony growth of *E. coli* cells with one copy of ClpP-mGFPmut3 (**A**: DHL747) and two copies of the ClpP-mGFPmut3 fusion (**B**: DHL987). The first copy corresponds to the endogenous *clpP* gene tagged with mGFPmut3. The second ClpP-mGFPmut3 copy was integrated in the *att*Tn7 site with expression controlled by the native *clpP* promoter (**Supplementary Note 2**). mCherry-ssrA was pulse-induced with IPTG for ~2 h and cells were spotted on an agar pad after washing away the IPTG. GFP images (green) were acquired every 25 min and RFP images every 5 min (data not shown). Cell growth and imaging was carried out at 30 ˚C. The ClpP-mGFPmut3 fusions show a relatively uniform distribution, although occasionally a weak punctate localization with dim foci can be seen (probably because mGFPmut3 is still not truly monomeric or some ClpP molecules are less mobile or even interact with the cell membrane). Bright fluorescent foci (as seen for e.g. with ClpP-Venus YFP, ClpP-sfGFP or ClpP-mCherry) were not observed. The scale bar (white) corresponds to 1 μm. The average GFP fluorescence per cell is approximately 2.0× as high for the strain with two copies of ClpP-mGFPmut3 (**D**: DHL987) as for the strain with just the endogenous *clpP* tagged with mGFPmut3 (**C**: DHL747). Data was pooled from 10 micro-colonies for each

strain. The GFP levels are corrected for cellular autofluorescence by imaging the MC4100 wildtype strain with the same GFP exposure time. The average GFP fluorescence per cell is in arbitrary units (a.u.).

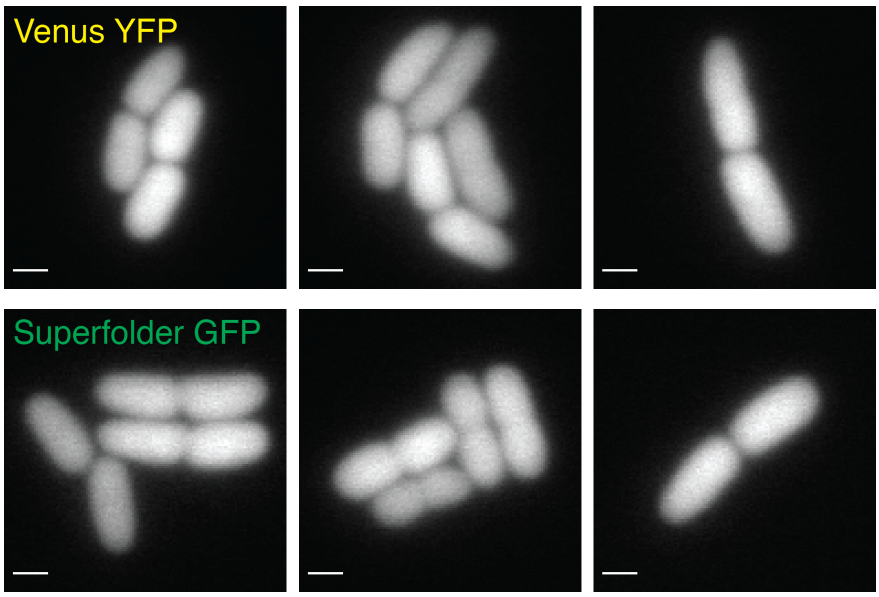

Supplementary Figure 5. Micrographs of *E. coli* cells expressing Venus YFP (upper row: DHL362) or superfolder GFP (lower row: DHL409) alone. The FP proteins are expressed from the strong P_{LlacO1} promoter on a pSC101 plasmid. FP foci or aggregates do not form despite high intracellular levels of the FP. The cells were grown at 37 ˚C to exponential phase, spread on an agar pad and then imaged at room temperature. The scale bar (white) corresponds to 1 μm.

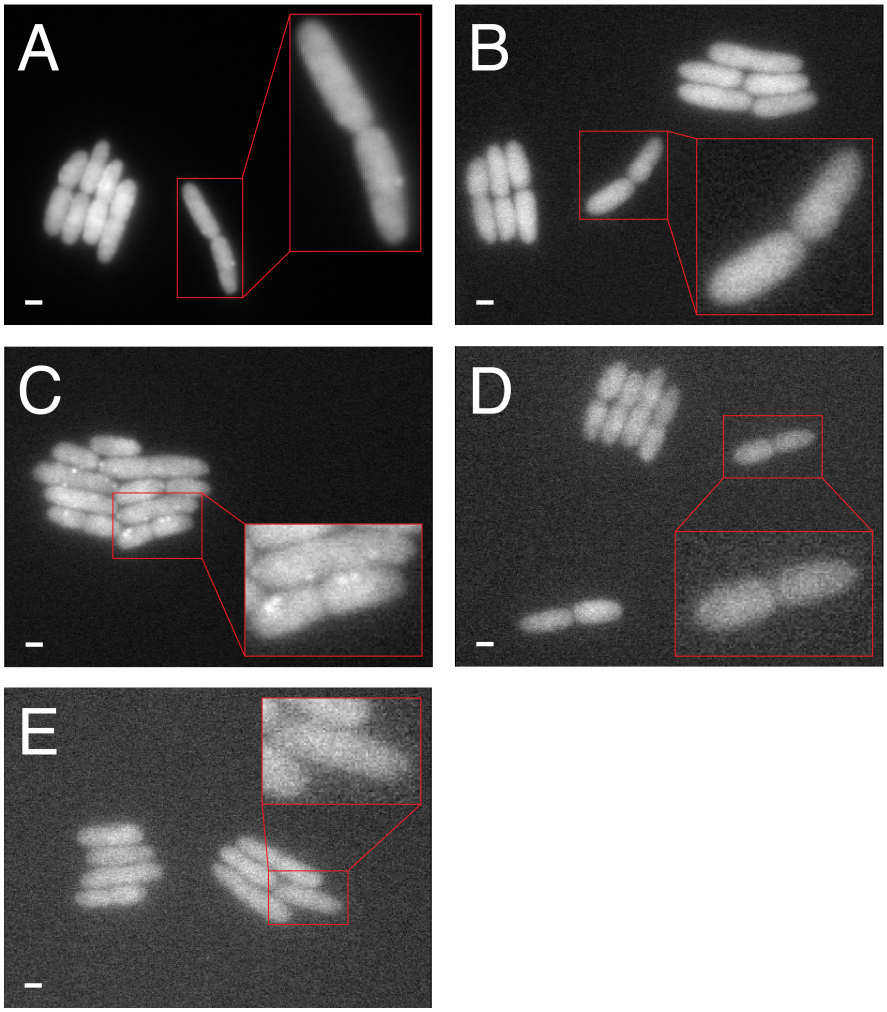

Supplementary Figure 6. False protein localization, caused by FP-mediated clustering, is a widespread phenomenon. Five proteins that reportedly form bright fluorescent foci based on the ASKA[3] and the Venus YFP[4] libraries were chosen and re-tagged with monomeric mGFPmut3. Bright fluorescent foci, resembling e.g. the ClpP-Venus YFP foci, were not observed for any of the tested fusion proteins. Over-night cultures of the corresponding strains were diluted 1:2,000, grown at 30 ˚C to exponential phase and imaged on agar pads with epi-fluorescence illumination. Still images were taken at room temperature and time-lapse movies of single cells growing into micro-colonies (**Supplementary Video 8**) were acquired at 30 ˚C. All strains were imaged in parallel with 1 s exposure time for GFP. For time-lapse imaging, GFP images were taken every 10 min. (**A**) The Hfq-mGFPmut3 fusion did not form foci but was found throughout the entire cell. This localization pattern is in agreement with published immunofluorescence[23] and electron microscopy[24] data. An occasional punctate localization with dim foci was observed (magnified cell or **Supplementary Video 8**). Even the brightest of the dim foci has less than 10% of the fluorescence intensity confined in the focus (data not shown), which is in strong contrast to a previously reported[4] 64.27% with an Hfq-Venus YFP fusion. (**B**) The PepP-mGFPmut3 fusion did not form fluorescent foci. (**C**) The IbpA-mGFPmut3 showed a punctate localization pattern but bright single foci were not observed. (**D**) The MviM-mGFPmut3 fusion did not form fluorescent foci. (**E**) The FruK-mGFPmut3 fusion did not form fluorescent foci. The displayed images were subjected to an individual min/max scaling. The scale bar (white) is 1 µm.

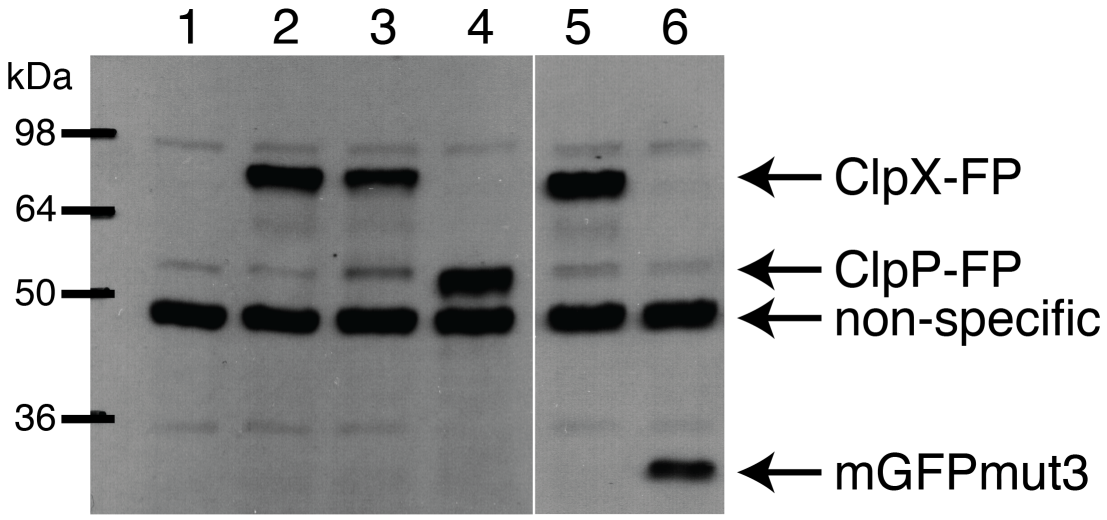

Supplementary Figure 7. Western blotting with anti-GFP antibody (**Supplementary Methods 1**) shows that the FP tag is not cleaved off. Probing with the anti-GFP antibody results in a non-specific band with a molecular weight (MW) below 50 kDa, which is present in the wildtype control (lane 1: MC4100) and all samples (lanes 2–6). mGFPmut3 (MW = 26.9 kDa) expressed alone (lane 6: DHL785) runs below the 36 kDa band of the molecular weight marker, as expected. ClpX-Venus YFP (lane 2: DHL466), ClpX-mGFPmut3 (lane 3: DHL620) and ClpX-PS-CFP2 (lane 5: DHL772) show a band of the expected size of a ClpX-FP fusion protein (MW = 73.2–73.4 kDa). ClpP-mGFPmut3 (lane 4: DHL661) has a band slightly above 50 kDa, corresponding to the expected size of the ClpP-mGFPmut3 fusion protein (MW = 50.3 kDa).

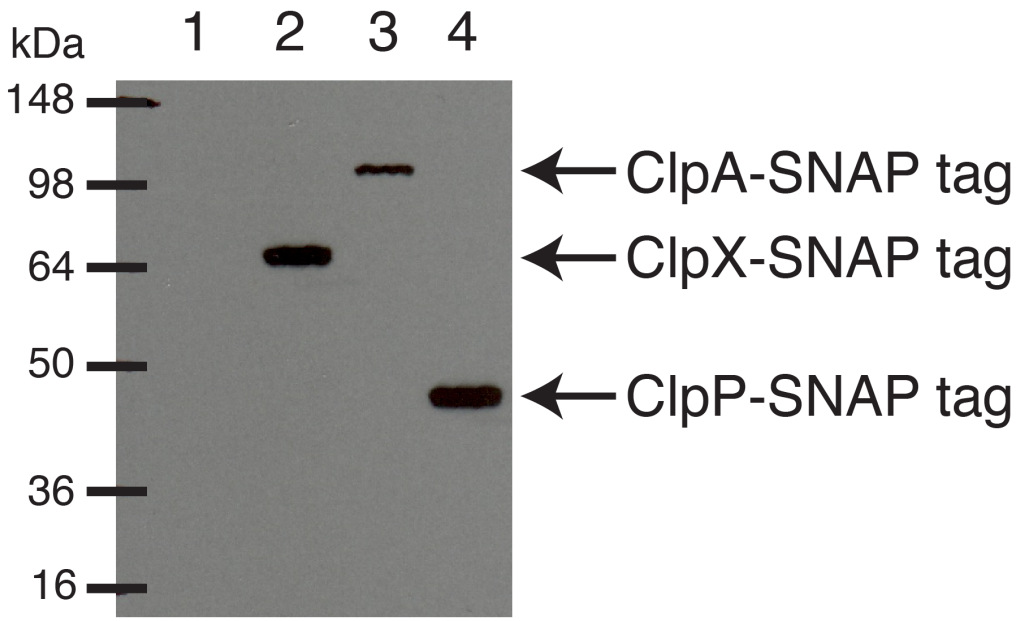

Supplementary Figure 8. Western blotting with anti-SNAP tag antibody (**Supplementary Methods 1**) shows that the SNAP tag is not cleaved off the fusion proteins. The anti-SNAP tag antibody does not cross-react with a native *E. coli* protein (lane 1: MC4100). ClpX-SNAP tag (lane 2: DHL624), ClpA-SNAP tag (lane 3: DHL659) and ClpP-SNAP tag (lane 4: DHL663) show a single band corresponding to the ClpX-SNAP tag (MW = 66.9 kDa), ClpA-SNAP tag (MW = 104.7 kDa) and ClpP-SNAP tag (MW = 43.7 kDa) fusion proteins, respectively. The band of the ClpA-SNAP tag (lane 3) is weak, probably because of less efficient transfer of the higher molecular-weight ClpA fusion protein onto the nitrocellulose membrane.

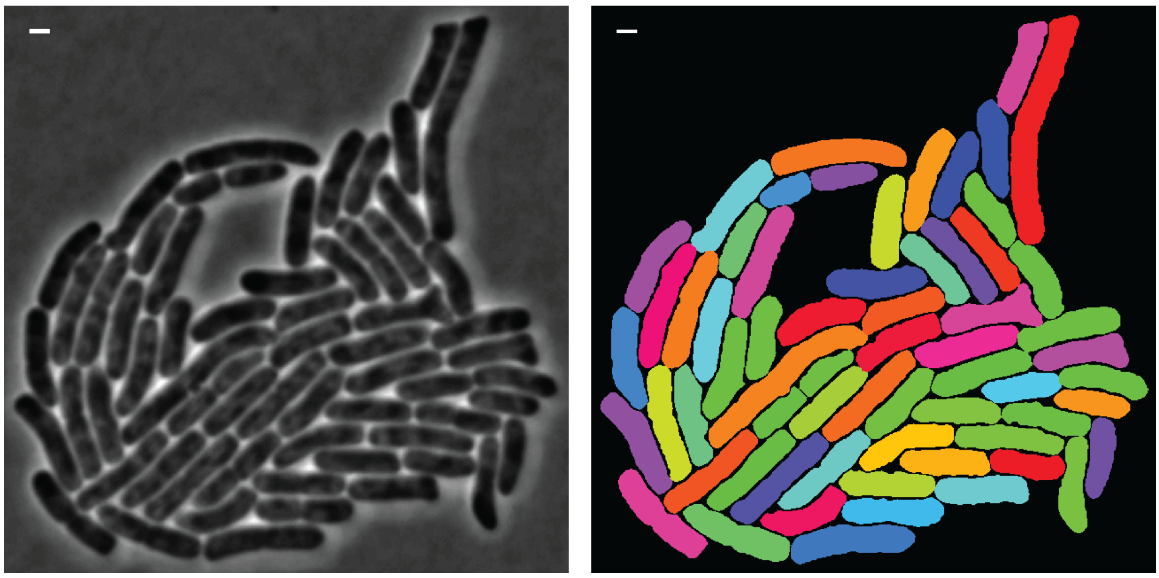

Supplementary Figure 9. Phase image (left) of a typical *E. coli* micro-colony grown on an agar pad under the microscope (100× magnification) and the corresponding segmentation mask (right, random color-coding). The phase image is 0.2–0.3 µm out-of-focus since individual *E. coli* cells are better separated in the out-of-focus image. The scale bar (white) corresponds to 1 µm.

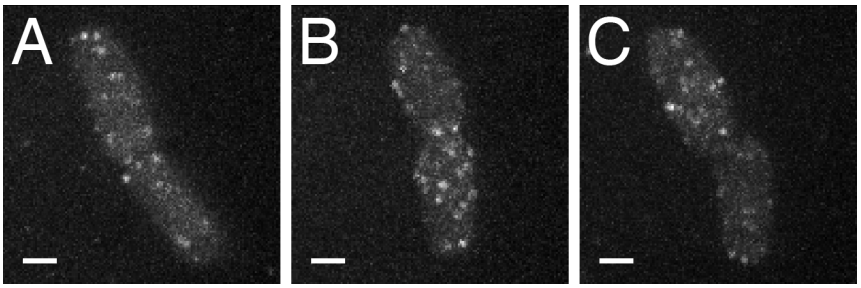

Supplementary Figure 10. ClpP-Dronpa molecules are uniformly distributed inside live *E. coli* cells. Individual *E. coli* cells harboring the ClpP-Dronpa fusion (DHL726) were imaged under constant illumination with a 488 nm laser (50 mW) in HILO mode and a time-series of 200 frames (30 ms exposure time, 250× magnification, no binning, 64 nm effective pixel size) was recorded. Dronpa molecules were not photo-converted with a 405 nm laser during the experiment. Cells were grown in imaging medium at 37 ˚C, confined between a coverslip and a microscope slide and imaged at room temperature. The maximum projection is shown for three different time-series (**A**–**C**). The scale bar (white) corresponds to 1 μm.

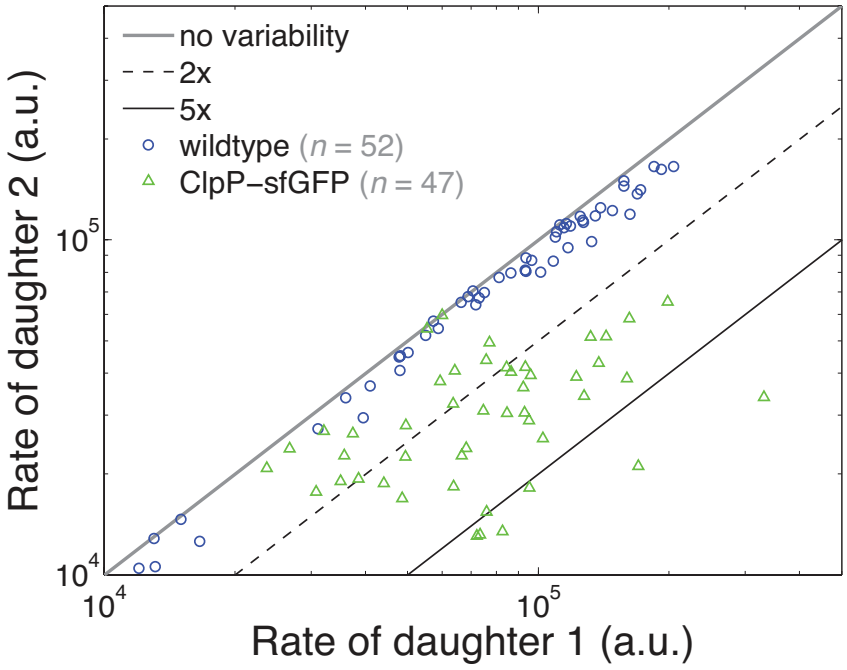

Supplementary Figure 11. ClpP-sfGFP foci (green triangles) still form and generate cell-to-cell variability at 30 ˚C. Cells were grown and imaged at 30 ˚C. The wildtype strain (blue circles) displays very low post-division cell-to-cell heterogeneity. Diagonal lines represent no cell-to-cell variability (gray line), 2× variability (dashed black line) and 5× variability (solid black line). Degradation rates are in arbitrary units (a.u.). The spread of the degradation rates along the diagonal is because of the pulse induction of the mCherry-ssrA degradation reporter and is not due to single-cell heterogeneity in protease levels or activity.

SUPPLEMENTARY TABLE 1

Name	Additional mutations	Amino acid sequence	Reference
mTagBFP	ΔE3	(SGGGGSNM)- SELIKENMHMKLYMEGTVDNHHFKCTSEGEG KPYEGTQTMRIKVVEGGPLPFAFDILATSFLY GSKTFINHTQGIPDFFKQSFPEGFTWERVTTYE DGGVLTATQDTSLQDGCLIYNVKIRGVNFTSN GPVMQKKTLGWEAFTETLYPADGGLEGRND MALKLVGGSHLIANIKTTYRSKKPAKNLKMP GVYYVDYRLERIKEANNETYVEQHEVAVARY CDLPSKLGHKLN	[25]
PS-CFP2	-	(SGGGG)- SKGAELFTGIVPILIELNGDVNGHKFSVSGEGE GDATYGKLTLKFICTTGKLPVPWPTLVATLSY GVQCFSRYPDHMKQHDFFKSAMPEGYIQERTI FFEDDGNYKTRAEVKFEGDTLVSRIELTGTDF KEDGNILGNKMEYNYNATNVYIVADKARNGI KVNFKVRHNIKDGSVQLADHYQQNTPIGDGP VLLPDNHYLSTQSALSKDPNEKRDHMIYLEFV TAAAITHGMDELYK	[26]
Superfolder GFP (sfGFP)	-	(SGGGG)- SKGEELFTGVVPILVELDGDVNGHKFSVRGEG EGDATNGKLTLKFICTTGKLPVPWPTLVTTLT YGVQCFSRYPDHMKQHDFFKSAMPEGYVQE RTISFKDDGTYKTRAEVKFEGDTLVNRIELKGI DFKEDGNILGHKLEYNFNSHNVYITADKQKN GIKANFKIRHNVEDGSVQLADHYQQNTPIGDG PVLLPDNHYLSTQSVLSKDPNEKRDHMVLLEF VTAAGITHGMDELYK	[27]
mGFPmut3	A206K[14]	(SGGGG)- SKGEELFTGVVPILVELDGDVNGHKFSVSGEG EGDATYGKLTLKFICTTGKLPVPWPTLVTTFG YGVQCFARYPDHMKQHDFFKSAMPEGYVQE RTIFFKDDGNYKTRAEVKFEGDTLVNRIELKG IDFKEDGNILGHKLEYNYNSHNVYIMADKQK NGIKVNFKIRHNIEDGSVQLADHYQQNTPIGD GPVLLPDNHYLSTQSKLSKDPNEKRDHMVLL EFVTAAGITHGMDELYK	This study
GFP(–30)	-	(SGGGG)- SKGEELFDGVVPILVELDGDVNGHEFSVRGEG EGDATEGELTLKFICTTGELPVPWPTLVTTLTY GVQCFSDYPDHMDQHDFFKSAMPEGYVQER TISFKDDGTYKTRAEVKFEGDTLVNRIELKGID FKEDGNILGHKLEYNFNSHDVYITADKQENGI	[28]

		KAEFEIRHNVEDGSVQLADHYQQNTPIGDGPV LLPDDHYLSTESALSKDPNEDRDHMVLLEFVT AAGIDHGMDELYK	
Dronpa	-	(SGGGGSN)- VIKPDMKIKLRMEGAVNGHPFAIEGVGLGKPF EGKQSMDLKVKEGGPLPFAYDILTTVFCYGN RVFAKYPENIVDYFKQSFPEGYSWERSMNYE DGGICNATNDITLDGDCYIYEIRFDGVNFPAN GPVMQKRTVKWEPSTEKLYVRDGVLKGDVN MALSLEGGGHYRCDFKTTYKAKKVVQLPDY HFVDHHIEIKSHDKDYSNVNLHEHAEAHSELP RQAK	[29]
rsFastLime	-	Dronpa with V157G	[30]
mEos2	-	(SGGGGSK)- SAIKPDMKIKLRMEGNVNGHHFVIDGDGTGK PFEGKQSMDLEVKEGGPLPFAFDILTTAFHYG NRVFAKYPDNIQDYFKQSFPKGYSWERSLTFE DGGICIARNDITMEGDTFYNKVRFYGTNFPAN GPVMQKKTLKWEPSTEKMYVRDGVLTGDIH MALLLEGNAHYRCDFRTTYKAKEKGVKLPG YHFVDHCIEILSHDKDYNKVKLYEHAVAHSG LPDNARR	[31]
Dendra2	-	(SGGGGSNMNTPGI)- NLIKEDMRVKVHMEGNVNGHAFVIEGEGKG KPYEGTQTANLTVKEGAPLPFSYDILTTAVHY GNRVFTKYPEDIPDYFKQSFPEGYSWERTMTF EDKGICTIRSDISLEGDCFFQNVRFKGTNFPPN GPVMQKKTLKWEPSTEKLHVRDGLLVGNIN MALLLEGGGHYLCDFKTTYKAKKVVQLPDA HFVDHRIEILGNDSDYNKVKLYEHAVARYSPL PSQVW	[32]
Venus YFP	V68L Q69M[33, 34]	(SGGGG)- SKGEELFTGVVPILVELDGDVNGHKFSVSGEG EGDATYGKLTLKLICTTGKLPVPWPTLVTTLG YGLMCFARYPDHMKRHDFFKSAMPEGYVQE RTIFFKDDGNYKTRAEVKFEGDTLVNRIELKG IDFKEDGNILGHKLEYNYNSHNVYITADKQKN GIKANFKIRHNIEDGGVQLADHYQQNTPIGDG PVLLPDNHYLSYQSALSKDPNEKRDHMVLLE FVTAAGITHGMDELYK	[35]
mVenus	A206K[14]	Venus YFP with A206K	[36]
mYPet	A206K[14]	(SGGGGSK)- GEELFTGVVPILVELDGDVNGHKFSVSGEGEG DATYGKLTLKLLCTTGKLPVPWPTLVTTLGY GVQCFARYPDHMKQHDFFKSAMPEGYVQER TIFFKDDGNYKTRAEVKFEGDTLVNRIELKGI DFKEDGNILGHKLEYNYNSHNVYITADKQKN GIKANFKIRHNIEDGGVQLADHYQQNTPIGDG PVLLPDNHYLSYQSKLFKDPNEKRDHMVLLE FLTAAGITEGMNELYK	[37, 38]

TagRFP-T	-	(SGGGGSK)- VSKGEELIKENMHMKLYMEGTVNNHHFKCTS EGEGKPYEGTQTMRIKVVEGGPLPFAFDILAT SFMYGSRTFINHTQGIPDFFKQSFPEGFTWERV TTYEDGGVLTATQDTSLQDGCLIYNVKIRGVN FPSNGPVMQKKTLGWEANTEMLYPADGGLE GRTDMALKLVGGGHLICNFKTTYRSKKPAKN LKMPGVYYVDHRLERIKEADKETYVEQHEVA VARYCDLPSKLGHKLN	[39]
mKate2	-	(SGGGGSK)- VSELIKENMHMKLYMEGTVNNHHFKCTSEGE GKPYEGTQTMRIKAVEGGPLPFAFDILATSFM YGSKTFINHTQGIPDFFKQSFPEGFTWERVTTY EDGGVLTATQDTSLQDGCLIYNVKIRGVNFPS NGPVMQKKTLGWEASTETLYPADGGLEGRA DMALKLVGGGHLICNLKTTYRSKKPAKNLK MPGVYYVDRRLERIKEADKETYVEQHEVAVA RYCDLPSKLGHR	[40]
mCherry	D8N	(SGGGG)- SKGEENNMAIIKEFMRFKVHMEGSVNGHEFEI EGEGEGRPYEGTQTAKLKVTKGGPLPFAWDI LSPQFMYGSKAYVKHPADIPDYLKLSFPEGFK WERVMNFEDGGVVTVTQDSSLQDGEFIYKVK LRGTNFPSDGPVMQKKTMGWEASSERMYPE DGALKGEIKQRLKLKDGGHYDAEVKTTYKA KKPVQLPGAYNVNIKLDITSHNEDYTIVEQYE RAEGRHSTGGMDELYK	[41]
mCherry2	-	mCherry (without D8N) with K97N K143C K74R S152T N201D T207L	N. Shaner (unpublished)
SNAP tag (SNAP26b)	-	(SGGGGSN)- MDKDCEMKRTTLDSPLGKLELSGCEQGLHEI KLLGKGTSAADAVEVPAPAAVLGGPEPLMQA TAWLNAYFHQPEAIEEFPVPALHHPVFQQESF TRQVLWKLLKVVKFGEVISYQQLAALAGNPA ATAAVKTALSGNPVPILIPCHRVVSSSGAVGG YEGGLAVKEWLLAHEGHRLGKPGLGPAGIGA PGS	17

Note: The amino acid sequence corresponding to the linker is surrounded by parentheses. For all FPs, the linker replaces the first methionine, which is encoded by the start codon.

Supplementary Table 2

Protein name	Protein function	Oligomerization state	ASKA library[3]	Venus YFP library[4] (Spot%_Protein)	Fusions with mGFPmut3 (this study)
Hfq	RNA chaperone	hexamer[42]	focus	64.27	mainly uniform with occasional dim foci
PepP	aminopeptidase	tetramer[43, 44]	focus	20.317	uniform
IbpA	small heat shock protein	polydisperse oligomers (100–150 subunits)[45]; fibrils *in vitro*[46]	focus	11.85	mainly uniform with some punctate foci
MviM	putative oxidoreductase	dimer* (PDB: 1TLT)	focus	8.828	uniform
FruK	fructose-1-phosphate kinase	dimer[47]*	focus	77.586	uniform

* The *in vivo* oligomerization status is not well studied.

SUPPLEMENTARY TABLE 3

Strains	Description	Antibiotic marker	Reference
MC4100	Wildtype (wt) *E. coli* strain	-	Silhavy lab
DH5α	Standard cloning strain	-	Silver lab
CNP154	MC4100 λφ(*rpoS750*-LacZ) Δ*clpX*::Kan	Kan	Silhavy lab
DHL193	MC4100 pKD46	Amp	This study
DHL362	MC4100 pPM16	Amp	This study
DHL409	DH5α pDHL409	Amp	This study
DHL436	MC4100 *clpP*-Venus YFP	-	This study
DHL440	MC4100 pDHL439	Amp	This study
DHL466	MC4100 *clpX*-Venus YFP-T1 terminator	-	This study
DHL476	DHL466 pDHL439	Amp	This study
DHL477	DHL466 pDHL468	Amp	This study
DHL481	MC4100 pDHL468	Amp	This study
DHL524	MC4100 *clpX*-mCherry2-T1 terminator	-	This study
DHL526	MC4100 *clpX*-sfGFP-T1 terminator	-	This study
DHL534	DHL526 pDHL439	Amp	This study
DHL537	DHL436 pDHL439	Amp	This study
DHL564	MC4100 Δ*clpX*::Kan	Kan	This study
DHL620	MC4100 *clpX*-mGFPmut3	-	This study
DHL622	MC4100 *clpX*-GFP(–30)	-	This study
DHL624	MC4100 *clpX*-SNAP tag	-	This study
DHL626	MC4100 *clpX*-Dronpa	-	This study
DHL657	MC4100 *clpA*-mGFPmut3	-	This study
DHL659	MC4100 *clpA*-SNAP tag	-	This study
DHL661	MC4100 *clpP*-mGFPmut3	-	This study
DHL663	MC4100 *clpP*-SNAP tag	-	This study
DHL708	MC4100 Δ*clpPX*	-	This study
DHL722	DHL708 pDHL439	Amp	This study
DHL726	MC4100 *clpP*-Dronpa	-	This study
DHL747	DHL661 pDHL439	Amp	This study
DHL771	MC4100 *clpX*-rsFastLime	-	This study
DHL772	MC4100 *clpX*-PS-CFP2	-	This study
DHL778	MC4100 *clpP*-sfGFP	-	This study
DHL780	MC4100 *clpP*-TagRFP-T	-	This study
DHL785	MC4100 Δ*clpX*::P_{clpX}-mGFPmut3	-	This study
DHL787	MC4100 *clpX*-mYPet	-	This study
DHL789	MC4100 *clpX*-TagRFP-T	-	This study
DHL805	DHL663 pDHL439	Amp	This study
DHL848	MC4100 *clpX*-mCherry-T1 terminator	-	This study
DHL922	MC4100 *hfq*-mGFPmut3	-	This study
DHL923	MC4100 *fruK*-mGFPmut3	-	This study
DHL925	MC4100 *mviM*-mGFPmut3	-	This study
DHL926	MC4100 *ibpA*-mGFPmut3	-	This study
DHL929	MC4100 *clpX*-mEos2	-	This study

DHL930	MC4100 *clpX*-mTagBFP	-	This study
DHL931	MC4100 *clpP*-mEos2	-	This study
DHL933	MC4100 *clpP*-Dendra2	-	This study
DHL944	MC4100 *pepP*-mGFPmut3	-	This study
DHL954	DHL726 pDHL439	Amp	This study
DHL955	DHL778 pDHL439	Amp	This study
DHL956	DHL933 pDHL439	Amp	This study
DHL986	DHL661 *att*Tn7::P_{clpPX}-*clpP*-mGFPmut3	-	This study
DHL987	DHL986 pDHL439	Amp	This study
DHL989	MC4100 *clpP*-mVenus YFP	-	This study
DHL990	MC4100 *clpP*-mKate2	-	This study
DHL991	MC4100 *clpP*-mYPet	-	This study
DHL993	MC4100 *clpP*-mCherry	-	This study

SUPPLEMENTARY TABLE 4

Plasmid	Description	Antibiotic marker	Reference
pBH27	pUC19-linker-mKate2 -FRT Kan FRT	Amp, Kan	M. El Karoui (unpublished)
pCP20	Yeast Flp recombinase expression plasmid.	Amp	[48]
pDHL18	pUC19-linker-YFP-T1 terminator	Amp	This study
pDHL19	pUC19-FRT Kan FRT	Amp, Kan	This study
pDHL146	pUC19-linker-Venus YFP-T1 terminator-FRT Kan FRT	Amp, Kan	This study
pDHL361	pUC19-mCherry2	Amp	This study
pDHL392	pUC19-linker-Venus YFP	Amp	This study
pDHL409	pSC101-P_{LlacO1}-sfGFP -T1 terminator	Amp	This study
pDHL411	pSC101-$P_{A1/O4}$-Venus YFP-ssrA(LAA) tag-T1 terminator	Amp	This study
pDHL414	pUC19-linker-Venus YFP-FRT Kan FRT	Amp, Kan	This study
pDHL424	pSC101-$P_{A1/O4}$-mCherry -ssrA(LAA) tag-T1 terminator	Amp	This study
pDHL439	pSC101-$P_{A1/O4}$-mCherry-ssrA(LAA) tag-T1 terminator-l*acI*^{q}	Amp	This study
pDHL445	pUC19-linker-mCherry	Amp	This study
pDHL446	pUC19-linker-mCherry2-T1 terminator	Amp	This study
pDHL458	pUC19-linker-sfGFP-T1 terminator	Amp	This study
pDHL468	pSC101-$P_{A1/O4}$-mCherry-T1 terminator-*lacI*^{q}	Amp	This study
pDHL470	pUC19-linker-mCherry-T1 terminator	Amp	This study
pDHL501	pUC19-linker-mCherry2-T1 terminator-FRT Kan FRT	Amp, Kan	This study
pDHL502	pUC19-linker-sfGFP-T1 terminator-FRT Kan FRT	Amp, Kan	This study
pDHL503	pUC19-linker-mCherry-T1 terminator-FRT Kan FRT	Amp, Kan	This study
pDHL580	pUC19-linker-mGFPmut3-FRT Kan FRT	Amp, Kan	This study
pDHL581	pUC19-linker-GFP(–30)-FRT Kan FRT	Amp, Kan	This study
pDHL582	pUC19-linker-SNAP tag-FRT Kan FRT	Amp, Kan	This study
pDHL583	pUC19-linker-Dronpa tag-FRT Kan FRT	Amp, Kan	This study
pDHL584	pUC19-linker-sfGFP-FRT Kan FRT	Amp, Kan	This study
pDHL677	pUC19-linker-PS-CFP2-FRT Kan FRT	Amp, Kan	This study
pDHL693	pUC19-linker-rsFastLime-FRT Kan FRT	Amp, Kan	This study
pDHL731	pUC19-linker-mYPet-FRT Kan FRT	Amp, Kan	This study
pDHL732	pUC19-linker-TagRFP-T-FRT Kan FRT	Amp, Kan	This study
pDHL843	pUC19-linker-mTagBFP-FRT Kan FRT	Amp, Kan	This study
pDHL844	pUC19-linker-mEos2-FRT Kan FRT	Amp, Kan	This study
pDHL851	pUC19-linker-Dendra2-FRT Kan FRT	Amp, Kan	This study
pDHL915	pUC19-linker-mCherry-FRT Kan FRT	Amp, Kan	This study
pDHL963	pUC19-linker-mVenus YFP-FRT Kan FRT	Amp, Kan	This study
pDHL970	pNDL1-P_{clpPX}-*clpP*-mGFPmut3	Amp	This study

pKD13	Template plasmid for gene deletions. The Kan resistance gene is flanked by FRT sites.	Amp, Kan	[48]
pKD46	Lambda Red recombinase expression plasmid.	Amp	[48]
pNDL1	pGRG25 with *att*P sites for Gateway cloning in the multiple cloning site, pSC101 *ori ts*	Amp	N. Lord (unpublished)
pPM1	pSC101-*rep101*(ts)-P_{LtetO1}-Venus YFP-T1 terminator	Amp	Lab collection
pPM14	pSC101-P_{LlacO1}-Venus YFP-ssrA(LAA) tag-T1 terminator	Amp	Lab collection
pPM16	pSC101-P_{LlacO1}-Venus YFP-T1 terminator	Amp	Lab collection
pPM88	pSC101-$P_{A1/O4}$-Venus YFP-T1 terminator-$lacI^q$	Amp	Lab collection
pUC19	High copy number cloning vector	Amp	Invitrogen

SUPPLEMENTARY TABLE 5

Primer	Sequence
DHL_P16_R	AAGG-CCCGGG-GGCGGATTTGTCCTACTCAGGAG
DHL_P17_F	CCTT-CCCGGG-GTGTAGGCTGGAGCTGCTTCGAAG
DHL_P18_R	GGAAGG-CCTGCAGG-CTGTCAAACATGAGAATTAATTCCGGG
DHL_P21_F	CCTT-GAGCTC-AGCGGTGGCGGTGGC-AGTAAAGGAGAAGAACTTTTCACTGGAGTTG
DHL_P80_k3	GCCCAGTCATAGCCGAATAGCC
DHL_P148_F	CG-GGATCC-ATGGTTAGTAAAGGAGAAGAAAATAACATGG
DHL_P149_R	GGAATTC-AAGCTT-ATGCGGTACCAGAACCTTTGTATAGTTC
DHL_P156_F	CG-GGATCC-ATGTCTAAAGGTGAAGAACTGTTCACCGG
DHL_P157_R	GGAATTC-AAGCTT-ATTTGTAGAGCTCATCCATGCCGTG
DHL_P158_F	AGCGGTGGCGGTGGCAGTAA
DHL_P159_R	ATTCCGGGGATCCGTCGACC
DHL_P165_R	AAGG-CCCGGG-TTATTTGTATAGTTCATCCATGCCATGTG
DHL_P170_F	AACCGTTGCTGATTTATGGCAAGCCGGAAGCGCAACAGGCATCTGGTGAA-AGCGGTGGCGGTGGCAGTAA
DHL_P171_R	GGAGATAAAATCCCCCCTTTTTGGTTAACTAATTGTATGGGAATGGTTAA-ATTCCGGGGATCCGTCGACC
DHL_P173_F	CTGAGTTTATTGGTCGTCTGCCGG
DHL_P174_R	CGTCAGTATATGGGGATGTTTCCCC
DHL_P175_R	GGAATTC-GACGTC-CTGCGGTACCAGAACCTTTGTATAGTTC
DHL_P178_F	CCTT-GAGCTC-AGCGGTGGCGGTGGC-AGTAAAGGAGAAGAAAATAACATGGCAATC
DHL_P179_R	GGAATT-AAGCTT-ATTTGTATAGTTCATCCATGCCACCAGTAC
DHL_P180_F	CCTT-GAGCTC-AGCGGTGGCGGTGGC-AGTAAGGGCGAGGAGGATAACATGGCC
DHL_P181_R	GGAATT-AAGCTT-ACTTGTACAGCTCGTCCATGC
DHL_P182_F	CTGAAGCGGTGGAATACGGTCTGGTCGATTCGATTCTGACCCATCGTAAT-AGCGGTGGCGGTGGCAGTAA
DHL_P183_R	AGCGTTGTGCCGCCCTGGATAAGTATAGCGGCACAGTTGCGCCTCTGGCA-ATTCCGGGGATCCGTCGACC
DHL_P184_F	TTTTTGCCTGCCGAATTCGC
DHL_P185_R	AGCTTGCGCACTTCATGCTGG
DHL_P186_F	CCTT-GAGCTC-AGCGGTGGCGGTGGC-AGTAAAGGTGAAGAACTGTTCACCGGTGTTG
DHL_P189_R	GGAATTC-AAGCTT-ATTTGTAGAGTTCATCCATGCCGTG
DHL_P215_F	TGACTTACGGATTCCAGAGTGCACAAAAGCACAAGGCGGAAGCAGCGCAT-AGCGGTGGCGGTGGCAGTAA
DHL_P216_R	CGTAACCTCTTTCGAGATTACGGACTTGACCAACCTACCTAACAATCAGA-ATTCCGGGGATCCGTCGACC
DHL_P237_F	CCG-CTCGAG-TTTACGCAGCATAACGCGCTAAATTC
DHL_P252_R	AAGG-CCCGGG-TTATTTGTATAGTTCATCCATGCCATGTG
DHL_P253_F	CCTT-GAGCTC-AGCGGTGGCGGTGGC-AGTAAAGGTGAAGAGCTGTTTGACGGTG

DHL_P254_R	AAGG-CCCGGG-TTACTTGTACAGCTCGTCCATTCCATG
DHL_P255_F	CCTT-GAGCTC-AGCGGTGGCGGTGGC-AGTAACGTGATTAAACCAGACATGAAGATCAAGC
DHL_P274_F	CCTT-GAGCTC-AGCGGTGGCGGTGGC-AGTAACATGGACAAAGATTGCGAAATGAAACG
DHL_P275_R	AAGG-CCCGGG-TTAGGAGCCTGGCGCGCCTATAC
DHL_P276_R	AAGG-CCCGGG-TTACTTGGCCTGCCTCGGCAG
DHL_P281_R	AAGG-CCCGGG-TTATTTGTAGAGTTCATCCATGCCGTG
DHL_P297_F	CCTT-GAGCTC-AGCGGTGGCGGTGGC-AGTAAAGGTGAAGAATTATTCACTGGTGTTGTC
DHL_P298_R	CCAGCCTACACCCGGGTTATTTGTAC
DHL_P306_F	CCTT-GAGCTC-AGCGGTGGCGGTGGC-AGTAAAGTGTCTAAGGGCGAAGAGCTGATTAAG
DHL_P307_R	AAGG-CCCGGG-TTAATTAAGTTTGTGCCCCAGTTTGCTAGG
DHL_P313_F	GCCAGGAAGCGCGTAACTGG
DHL_P314_R	CAGTGAACATGGTGGGCGGG
DHL_P321_F	CCTT-GAGCTC-AGCGGTGGCGGTGGC-AGTAAAAGTGCGATTAAGCCAGACATGAAGATC
DHL_P322_R	AAGG-CCCGGG-TTATCGTCTGGCATTGTCAGGCAATC
DHL_P336_F	TTACAATCGGTACAGCAGGTTTTTTCAATTTTATCCAGGAGACGGAAATG-ATTCCGGGGATCCGTCGACC
DHL_P337_R	TGGTTAACTAATTGTATGGGAATGGTTAATTATTCACCAGATGCCTGTTG-TGTAGGCTGGAGCTGCTTCG
DHL_P346_F	GGC-AACATGGCTCTGTCGCTTGAAGG
DHL_P347_R	ATCACCCTTCAGCACTCCATCACG
DHL_P375_F	TTGCGTCGTCGTGTGCGGCACAAAGAACAAAGAAGAGGTTTTGACCCATG-AGTAAAGGAGAAGAACTTTTCACTGGAGTTG
DHL_P440_F	CCTT-GAGCTC-AGCGGTGGCGGTGGC-AGTAAGGGCGCCGAGCTGTTCAC
DHL_P441_R	AAGG-CCCGGG-TTACTTGTACAGCTCATCCATGCCG
DHL_P449_F	CCTT-GAGCTC-AGCGGTGGCGGTGGC-AGTAACATGAGCGAGCTGATTAAGGAGAACATG
DHL_P450_R	AAGG-CCCGGG-TTAATTAAGCTTGTGCCCCAGTTTGC
DHL_P453_F	CCTT-GAGCTC-AGCGGTGGCGGTGGC-AGTAACATGAACACACCGGGAATTAACC
DHL_P454_R	AAGG-CCCGGG-TTACCACACCTGGCTGGGCAGG
DHL_P472_R	AAGG-CCCGGG-TTATTTGTATAGTTCATCCATGCCACCAGTAC
DHL_P496_F	GTAGCAGCGCGCAGAATACTTCCGCGCAACAGGACAGCGAAGAAACCGAA-AGCGGTGGCGGTGGCAGTAA
DHL_P497_R	CGGGGAACGCAGGATCGCTGGCTCCCCGTGTAAAAAAACAGCCCGAAACC-ATTCCGGGGATCCGTCGACC
DHL_P498_F	GTCCGCAGTTGGCCGCAATGATGGCGCGCGTCGACTTACAACCTTTTAAC-AGCGGTGGCGGTGGCAGTAA
DHL_P499_R	CGAGATTAGCGTCAATAATCAGCAGCGTTTTCATTATGCCTCTCCTGCTG-ATTCCGGGGATCCGTCGACC
DHL_P500_F	TGAAAAAGCCGGAAGAAATCGAAGCGTTGATGGTTGCTGCGAGAAAGCAA-AGCGGTGGCGGTGGCAGTAA
DHL_P501_R	GGAAATAGCCAGCGCCAGCGTCGCGCCCGCCATGCCGCCACCGACGATGATTACGCTCAT-ATTCCGGGGATCCGTCGACC

DHL_P504_F	TGCTGGCGCAACGTATCGTTGACAAGATCTGGCGCGATGCGATGAGT GAA-AGCGGTGGCGGTGGCAGTAA
DHL_P505_R	AATAGTCTACCTGGATTATGGTGAATTGCTACCGCCAGATGTTACAGG GT-ATTCCGGGGATCCGTCGACC
DHL_P506_F	TCGAACGCGTGATTCCGGAAGCGAAAAAACCGCGCCGTATCGAAATC AAC-AGCGGTGGCGGTGGCAGTAA
DHL_P507_R	CCTGACGGCGAGCATGGAGATGTCAGGCCGCGCCAGGCGGCCTTAGG GAA-ATTCCGGGGATCCGTCGACC
DHL_P518_F	AAGGAAAAGAGAGAATGGCTAAGGGG
DHL_P519_R	CTTCCGCAATTTCAACTGCTTTACC
DHL_P520_F	GAATGGATCGCCAAACCACCG
DHL_P521_R	TCAGGAACAGCTCAGGGTGCG
DHL_P522_F	GACTGGATGTCCATGACGTGGG
DHL_P523_R	CTGACATGCACGGTGGTGATGG
DHL_P526_F	GTCAGCGTGAAACCGTGCAGG
DHL_P527_R	CGTAACAAGTTAGGAAGTTTAAAAGCGACG
DHL_P528_F	GCATTGCTATCGCTGTGGCTGG
DHL_P529_R	TTTTCTCAATGTTGTACGGCGGG
DHL_P550_F	GTCACGACGTTGTAAAACGACGGCCAGTGAATTCGAGCTCAGCGGTG GCGGTGGCAGTAA
DHL_P551_R	TCTCTTTTCGTTGGGATCTTTCGAAAGTTTAGATTGATAGGACAGGTA ATGGTTGTCTGG
DHL_P552_F	ACCAGACAACCATTACCTGTCCTATCAATCTAAACTTTCGAAAGATCC CAACGAAAAGAG
DHL_P553_R	ACTTCGAAGCAGCTCCAGCCTACACCCCGGGTTATTTGTATAGTTCAT CCATGCCATGTG
DHL_P556_R	ATGACACGACTGTGCTTCACGC
DHL_P557_F	GGGG-ACAAGTTTGTACAAAAAAGCAGGCTCT-CGCAGCATAACGCGCTAAATTCG
DHL_P558_R	GGGG-ACCACTTTGTACAAGAAAGCTGGGTC-ATTCCGGGGATCCGTCGACC
M13_R	CAGGAAACAGCTATGACC
NL15_F	CTGGTTGGTCGACACTAGTATTACCC
NL32_R	GATGACGGTTTGTCACATGGA
NL35_F	CCCCTATAGTGAGTCGTATTACATGG
NL73_R	GGATTCATCGACTGTGGCCG

Supplementary Note 1

Descriptions of Supplementary Videos 1–8

Supplementary Video 1. ClpP-Venus YFP forms bright fluorescent foci in live *E. coli* cells. The ClpP-Venus YFP foci are not present in all cells, the foci localize preferentially to the cell poles and mid-cell region and show binary segregation at cell division. Cells without a focus have a cytoplasmic YFP signal (not visible in this movie) and usually form a YFP focus in the next cell cycles. A few ClpP-Venus YFP foci appear blurred because they are in different focal planes (z-stacks are required to detect all foci in a micro-colony, data not shown). Some cells have small foci, which are very faint and barely visible in the movie. The YFP images of this movie were acquired with 2 × 2 binning (effective pixel size is 129 nm). The cell boundary (red) was determined by segmenting the respective phase images. The scale bar (white) corresponds to 1 µm. The movie is part of a dual-color experiment; see **Supplementary Video 2** for the corresponding RFP movie.

Supplementary Video 2. Degradation of an mCherry-ssrA reporter in the ClpP-Venus YFP strain shows that the ClpP-Venus YFP foci generate post-division cell-to-cell variability. The synthesis of mCherry-ssrA was pulse-induced before the cells were monitored. The RFP images were subjected to a "per-frame auto-scaling" to better display the post-division variability between daughter cells. The foci in the RFP image are not due to spectral bleedthrough from the ClpP-Venus YFP foci but probably represent immortal mCherry molecules bound to the ClpP-FP foci (**Supplementary Fig. 1**). The RFP images of this movie were acquired with 2 × 2 binning (effective pixel size is 129 nm). The cell boundary (red) was determined by segmenting the respective phase images. The scale bar (white) corresponds to 1 µm. The movie is part of a dual-color experiment; see **Supplementary Video 1** for the corresponding YFP movie.

Supplementary Video 3. Degradation of the mCherry-ssrA reporter displays very little post-division variability in the wildtype strain (protease is not tagged with an FP). The mCherry-ssrA reporter was pulse-induced before imaging. mCherry-ssrA is specifically degraded by ClpXP and ClpAP. The RFP images were per-frame auto-scaled to better illustrate the low degree of variability after cell division. The YFP images of this movie were acquired with 2 × 2 binning (129 nm effective pixel size). The cell boundary (red) was determined by segmenting the respective phase images. The scale bar (white) corresponds to 1µm.

Supplementary Videos 4–7. HILO microscopy of cells expressing ClpA-mGFPmut3, ClpP-mGFPmut3 and ClpX-mGFPmut3 (**Supplementary Videos 4–6**, respectively). Cells have ~50 particles, which are not localized in a foci but in fact move rapidly and seem to sample the entire cell. mGFPmut3 expressed alone (i.e., not fused to another protein) from the P_{clpX} promoter at the endogenous locus displays a uniform cytoplasmic distribution (**Supplementary Video 7**). HILO imaging was performed as described (see **Online Methods**). The scale bar (white) is 1 µm. The images of the movie sequences were subjected to a quantitative grayscale scaling (left) and to a "per-frame auto-scaling" (right) to better display the particle movement despite fast photo-bleaching (see **Online Methods**).

Supplementary Video 8. Time-lapse microscopy of *E. coli* strains with the Hfq-mGFPmut3, PepP-mGFPmut3, IbpA-mGFPmut3, MviM-mGFPmut3, and FruK-mGFPmut3 fusions, respectively. The fusions are constructed at the endogenous gene loci. Cells were grown to exponential phase in imaging medium and micro-colony growth was filmed on an agar pad with exposures every 10 min. Cell growth and imaging was performed at 30 ˚C. GFP images with 1 sec exposure time were acquired every 10 min. The GFP images of the movies were acquired with no binning (effective pixel size is 64.5 nm). The scale bar (white) corresponds to 1 µm. The GFP images of the movie sequences were subjected to a quantitative grayscale scaling.

Supplementary Note 2

***E. coli* strains**

All *E. coli* strains used in this study are listed in **Supplementary Table 3.**

The FP fusions to *clpA*, *clpP* and *clpX* were constructed at the endogenous chromosomal locus with the lambda Red-mediated homologous recombination method[48]. Primers containing 50 nucleotide upstream or downstream homology to the integration site (*clpA*: DHL_P215_F and DHL_P216_R, *clpP*: DHL_P182_F and DHL_P183_R and *clpX*: DHL_P170_F and DHL_P171_R) were used to amplify the integration cassettes with the polymerase chain reaction (PCR) and AccuPrime Pfx (Invitrogen) or Phusion (Finnzymes) DNA polymerases. The PCR products were purified, digested with DpnI (NEB) and electroporated into *E. coli* strain DHL193 (MC4100 pKD46). Cells were resuspended in SOC media supplemented with 0.2% (w/v) arabinose, grown for 2 h at 30 ˚C (or 2 h at 30 ˚C followed by overnight incubation at room temperature) and spread on agar plates containing 30 µg/ml Kanamycin. Resistant colonies were isolated by restreaking and the presence of the integration cassette was confirmed by colony PCR (http://openwetware.org/wiki/Knight:Colony_PCR). Two different primer sets, one for the upstream and one for the downstream integration scar, were used to confirm the site-specific integration of the FP cassette. For both primer sets, one primer binds to the genome and the other one to the integration cassette (*clpA*_upstream: DHL_P313_F and NL73_R, *clpA*_downstream: DHL_P80_k3 and DHL_P314_R, *clpP*_upstream: DHL_P184_F and NL73_R, *clpP*_downstream: DHL_P80_k3 and DHL_P185_R, *clpX*_upstream: DHL_P173_F and NL73_R and *clpX*_upstream: DHL_P80_k3 and DHL_P174_R or primers DHL_P80_k3 and DHL_P556_R) and hence give no band for the wildtype strain. Plasmid pKD46 was eliminated from positive clones by growing the cells at 42 ˚C. Loss of the pKD46 plasmid was confirmed by testing the cells for sensitivity to ampicillin. The integrated FP cassette was then P1 transduced into a fresh MC4100 strain using standard methods (http://openwetware.org/wiki/Sauer:P1vir_phage_transduction) followed by selection for kanamycin resistance on agar plates. The FRT-flanked Kan resistance marker cassette was then eliminated by transforming the cells with plasmid pCP20 and selection on agar plates with 100 µg/ml ampicillin at 30 ˚C. Elimination of the Kan marker, which leaves behind an 88 bp scar downstream of the stop codon of the FP, was verified by PCR with gene-specific primers (*clpA*: DHL_P313_F and DHL_P314_R, *clpP*: DHL_P184_F and DHL_P185_R and *clpX*: DHL_P173_F and DHL_P174_R or primers DHL_P173_F and DHL_P556_R) and sequence-verified (Genewiz or in-house facility) with the same primer sets. Strains were also checked for sensitivity to kanamycin. Plasmid pCP20 was eliminated by growing the cells at 42 ˚C. Loss of the temperature-sensitive pCP20 plasmid was validated by testing for ampicillin sensitivity.

The following plasmids were used as PCR templates for constructing the chromosomal FP integrations to *clpA*, *clpP* and *clpX*: pDHL414 for DHL436, pDHL146 for DHL466, pDHL501 for DHL524, pDHL502 for DHL526, pDHL580 for DHL620, pDHL581 for DHL622, pDHL582

for DHL624, pDHL583 for DHL626, pDHL580 for DHL657, pDHL582 for DHL659, pDHL580 for DHL661, pDHL582 for DHL663, pDHL583 for DHL726, pDHL693 for DHL771, pDHL677 for DHL772, pDHL584 for DHL778, pDHL732 for DHL780, pDHL731 for DHL787, pDHL732 for DHL789, pDHL503 for DHL848, pDHL844 for DHL929, pDHL843 for DHL930, pDHL844 for DHL931, pDHL851 for DHL933, pDHL963 for DHL989, pBH27 for DHL990, pDHL731 for DHL991, and pDHL915 for DHL993.

Strain DHL564 was built by P1 transducing the Δ*clpX*::Kan allele from CNP154 into MC4100 and selection on agar plates containing 30 µg/ml kanamycin.

Strain DHL708 was built by deleting the *clpPX* operon with lambda-Red mediated homologous recombination (see above for details). The FRT-flanked Kan cassette was PCR amplified from pKD13 with primers DHL_P336_F and DHL_P337_R and transformed into DHL193. The Δ*clpPX* region was PCR amplified with primers DHL_P237_F and DHL_P174_R and the PCR product was sequenced.

Strain DHL785 was built by amplifying mGFPmut3 from pDHL580 with primers DHL_P375_F and DHL_P171_R and transforming the PCR product into strain DHL193 to replace the *clpX* coding region with mGFPmut3 by lambda-Red mediated homologous recombination. Expression of mGFPmut3 is hence under control of the endogenous P_{clpX} promoter in a Δ*clpX* background. The P_{clpX}-mGFPmut3 part was amplified with primers DHL_P184_F and DHL_P174_R, the PCR product was purified and the regions containing the integration scars where sequenced with primers DHL_P184_F and DHL_P174_R.

Plasmid pDHL580 was used as the PCR template for constructing the integration cassettes to tag *hfq*, *fruK*, *mviM*, *ibpA* and *pepP* with mGFPmut3, resulting in strains DHL922, DHL923, DHL925, DHL926 and DHL944. The strains were constructed according to the lambda-Red protocol described above. Chromosomal integration was verified with two gene-specific primer sets, where one primer binds to the genome and the other primer to the integration cassette (*hfq*_upstream: DHL_P518_F and NL73_R, *hfq*_downstream: DHL_P80_F and DHL_P519_R, *fruK*_upstream: DHL_P520_F and NL73_R, *fruK*_downstream: DHL_P80_F and DHL_P521_R, *mviM*_upstream: DHL_P526_F and NL73_R, *mviM*_downstream: DHL_P80_F and DHL_P527_R, *ibpA*_upstream: DHL_P528_F and NL73_R, *ibpA*_downstream: DHL_P80_F and DHL_P529_R, *pepP*_upstream: DHL_P522_F and NL73_R and *pepP*_downstream: DHL_P80_F and DHL_P523_R). Verified integration cassettes were P1 transduced into MC4100 and the FRT-flanked Kan resistance cassette was removed. The integration sites were sequenced (Genewiz) with gene-specific primers (*hfq*: DHL_P518_F and DHL_P519_R, *fruK*: DHL_P520_F and DHL_P521_R, *mviM*: DHL_P526_F and DHL_P527_R, *ibpA*: DHL_P528_F and DHL_529_R and *pepP*: DHL_P522_F and DHL_P523_R).

Strain DHL986 was built by integrating a second copy of P_{clpPX}-*clpP*-mGFPmut3 in the *att*Tn7 site of strain DHL661 with a method previously described[49]. In short, strain DHL661 was transformed with plasmid pDHL970 and grown at 30 ˚C on Amp plates. Single colonies were isolated and the plasmid was eliminated by growth at 42 ˚C. Plasmid loss was confirmed by testing for ampicillin sensitivity. Chromosomal integration was verified by PCR with primers NL32_R and NL35_F. The fluorescence intensity of strain DHL986 is twice as high as the fluorescence intensity of DHL661 as expected for a strain that has two gene copies of *clpP*-mGFPmut3 (**Supplementary Fig. 4**).

Plasmids

All plasmids are listed in **Supplementary Table 4**.

Plasmid constructions were verified by analytical restriction digests. All cloning steps that involved PCR amplification were validated by DNA sequencing. Vent (NEB) or Phusion (Finnzymes) polymerases were used for standard cloning. All restriction enzymes were purchased from NEB and used according to the manufacturer's instructions.

Two types of plasmids were used for constructing the chromosomal FP fusions to *clpA*, *clpP* and *clpX*. Both plasmids were derived from the same ancestor (pDHL19) and are identical except that one carries the linker-FP alone and the other one carries the linker-FP followed by the T1 transcriptional terminator. All FP tagging vectors share the same primer binding sites for amplifying the FP-FRT Kan FRT integration cassettes. The forward primer binding site (see DHL_P158_F for sequence) corresponds to the linker region and the reverse primer binding site (see DHL_P159_R for sequence) is downstream of the FRT-flanked Kan marker.

pDHL19 was built by amplifying the FRT-flanked kanamycin resistance marker cassette (FRT Kan FRT) from pKD13 with primers DHL_P17_F and DHL_P18_R, the PCR product was digested with XmaI and SbfI and ligated into pUC19, which was cut with the same restriction enzymes.

pDHL146 was built in two steps. Venus YFP was amplified from pPM1 with primers DHL_P21_F and DHL_P16_R, the PCR product was digested with SacI and XmaI and ligated into pUC19, which was cut with the same enzymes. The resulting plasmid, named pDHL18, was digested with SacI and XmaI and the linker-Venus YFP-T1 terminator fragment was purified and ligated into SacI/XmaI-digested pDHL19. The Venus YFP variant used here contains two additional mutations (V68L, Q69M) from Citrine YFP[33, 34]. These two mutations are known to be beneficial to Citrine YFP.

pDHL409 was built by amplifying superfolder GFP (sfGFP) from pHC467 (courtesy of Prof. T. Bernhardt, Harvard Medical School) with primers DHL_P156_F and DHL_P157_R, digested with BamHI and HindIII and ligated into pPM16, which was also digested with the same enzymes. This puts expression of sfGFP under the control of the P_{LlacO1} promoter[50], which is constitutively 'ON' in MC4100 (since this strains lacks *lacI*). pPM16 harbors a pSC101 origin and the *bla* gene for Amp resistance.

pDHL414 was built in two steps. First, Venus YFP was amplified from pPM1 with primers DHL_P21_F and DHL_P165_R, digested with SacI and XmaI and subcloned into pUC19 cut with the same enzymes. The resulting plasmid, pDHL392, was digested with SacI and XmaI and the SacI-linker-Venus YFP-XmaI fragment was purified and ligated into pDHL19, which was also cut with SacI and XmaI.

pDHL439 was built in three steps. First, pPM88 was digested with XhoI and EcoRI to cut out the $P_{A1/O4}$ promoter[51]. The DNA fragment was purified and ligated into XhoI/EcoRI-cut pPM14, resulting in plasmid pDHL411. Second, mCherry without the stop codon was amplified from BioBrick Z0075[52] with primers DHL_P148_F and DHL_P175_R, digested with BamHI and AatII and ligated into pDHL411, which was digested with the same enzymes. The resulting plasmid, named pDHL424, was digested with XhoI and XbaI, the fragment corresponding to $P_{A1/O4}$-mCherry-ssrA(LAA) was purified and ligated into pPM88, which was also digested with XhoI and XbaI. pPM88 has a pSC101 origin, the *bla* gene and $lacI^q$. The ssrA(LAA) tag is the native *E. coli* ssrA tag with the following amino acid sequence: AANDENYALAA[53, 54].

pDHL468 was derived from pDHL439 by exchanging the mCherry-ssrA(LAA) fragment for mCherry. mCherry was PCR amplified from pDHL439 with primers DHL_P148_F and DHL_P149_R, digested with BamHI and HindIII and ligated into pDHL439, which was digested with the same enzymes.

pDHL501 was built in two steps. Primers DHL_P180_F and DHL_P181_R were used to amplify mCherrry2 from pDHL361. mCherry2 was synthesized by GenScript (DNA sequence courtesy of Dr. N. Shaner). The PCR product was digested with SacI and HindIII. Next, pDHL18 was digested with HindIII and the HindIII-T1 terminator-HindIII part was purified. The SacI-linker-mCherry-HindIII and the HindIII-T1 terminator-HindIII fragments were subcloned into SacI/HindIII-digested pUC19 resulting in plasmid pDHL446. The linker-mCherry2-T1 terminator fragment was then cut out of pDHL446 with SacI and XmaI and ligated into SacI/XmaI-cut pDHL19.

pDHL502 was built in two steps. First, primers DHL_P186_F and DHL_P189_R were used to amplify sfGFP from pDHL409. Primer DHL_P189_R introduces a silent mutation into the C-terminus of sfGFP to eliminate an existing SacI site. The PCR product and pDHL18 were digested with SacI and HindIII. The digested PCR product, the HindIII-T1 terminator-HindIII fragment and the pDHL18 backbone were purified and combined in a triple ligation and the resulting plasmid was named pDHL458. The linker-sfGFP-T1 terminator fragment was then cut out from pDHL458 with SacI and XmaI and ligated into pDHL19, also cut with SacI and XmaI.

pDHL503 was built in two steps. Primers DHL_P178_F and DHL_P179_R were used to amplify mCherry from BioBrick Z0075[52], the PCR product was digested with SacI and HindIII and subcloned into SacI/HindIII-digested pUC19 giving plasmid pDHL445. The mCherry in Z0075 already contained the D8N mutation. Next, pDHL18 was digested with HindIII and the HindIII-T1 terminator-HindIII part was purified. Vector pDHL445 was cut with SacI and HindIII, the linker-mCherry insert was purified and subcloned together with the T1 terminator part into SacI/HindIII-digested pDHL18. The resulting plasmid was named pDHL470. The linker-mCherry-T1 terminator fragment was released from pDHL470 by digestion with SacI and XmaI and ligated into SacI/XmaI-digested pDHL19.

pDHL580 was built in a single step. mGFPmut3 was amplified from pDH78 (D. Huh and J. Paulsson, manuscript in preparation) with primers DHL_P21_F and DHL_P252_R, digested with SacI and XmaI and ligated into pDHL19, which was also digested with SacI and XmaI. mGFPmut3 corresponds to GFPmut3[55] with the A206K[14] mutation.

pDHL581 was built by PCR amplifying GFP(–30) from pET-GFP-NEG30[28] with primers DHL_P253_F and DHL_P254_R, digested with SacI and XmaI and ligated into pDHL19, which was digested with the same enzymes.

pDHL582 was built by amplifying the SNAP tag from the pSNAP-tag(T7) plasmid (NEB, cat.# N9174S) with primers DHL_P274_F and DHL_P275_R. The PCR product was digested with SacI and XmaI and ligated into SacI/XmaI-digested pDHL19.

pDHL583 was built by amplifying Dronpa from pcDNA3-Dronpa (courtesy of Dr. H. Zhong, Janelia Farm) with primers DHL_P255_F and DHL_P276_R, digested with SacI and XmaI and ligated into pDHL19, which was also digested with SacI and XmaI.

pDHL584 was built by amplifying sfGFP from pDHL502 with primers DHL_P186_F and DHL_P281_R. Primer DHL_P281_R introduces a silent mutation into the C-terminus of sfGFP to eliminate an existing SacI site. The PCR product was digested with SacI and XmaI and ligated into pDHL19, which was digested with the same enzymes.

pDHL677 was built by amplifying PS-CFP2 from pPS-CFP2-N (Evrogen, cat.# FP802) with primers DHL_P440_F and DHL_P441_R, digested with SacI and XmaI and ligated into SacI/XmaI-digested pDHL19.

pDHL693 was built in two steps. First, primers DHL_P346_F and DHL_P347_R were used to introduce the V157G mutation in plasmid pET15b-Dronpa-AP tag (lab collection) with ‘Round-

the-horn site-directed mutagenesis (http://openwetware.org/wiki/'Round-the-horn_site-directed_mutagenesis) and Phusion (Finnzymes) DNA polymerase. The resulting vector was used as the PCR template to amplify rsFastLime (i.e., Dronpa V157G) with primers DHL_P255_F and DHL_P276_R. The PCR product was then digested with SacI and XmaI and ligated into pDHL19, which was also cut with SacI and XmaI.

pDHL731 was built by amplifying mYPet from pROD50[38] (i.e., pUC-11aa-mYPet-kan) with primers DHL_P297_F and DHL_P298_R, digested with SacI and XmaI and ligated into pDHL19, which was cut with the same enzymes. mYPet corresponds to YPet with the A206K[14] mutation.

pDHL732 was built by amplifying TagRFP-T from pmTagRFP-T-Tubulin-6 (courtesy of Prof. M. Davidson, Florida State University) with primers DHL_P306_F and DHL_P307_R, digested with SacI and XmaI and ligated into pDHL19, which was also digested with SacI and XmaI.

pDHL843 was built by PCR amplifying mTagBFP (courtesy of Prof. M. Springer, Harvard Medical School) with primers DHL_P449_F and DHL_P450_R. The PCR product was digested with SacI and XmaI and ligated into pDHL19, which was also cut with SacI and XmaI.

pDHL844 was built by amplifying mEos2 from pRsetA-mEos2[31] with primers DHL_P321_F and DHL_P322_R, digested with SacI and XmaI and ligated into SacI/XmaI-digested pDHL19.

pDHL851 was built by PCR amplifying Dendra2 from plasmid pDendra2-Tubulin (courtesy of Sophie Dumont, Harvard Medical School) with primers DHL_P453_F and DHL_P454_R. The insert was digested with SacI and XmaI and then ligated into SacI/XmaI-digested pDHL19.

pDHL915 was built by amplifying mCherry from pDHL503 with primers DHL_P178_F and DHL_P472_R. The PCR product was digested with SacI and XmaI and ligated into pDHL19, which was cut with the same restriction enzymes.

pDHL963 was built in two steps. First, Venus YFP part 1 (aa# 2–205) was amplified from pDHL414 with primers DHL_P550_F and DHL_P551_R and Venus YFP part 2 (aa# 207–238) was amplified from pDHL414 with primers DHL_P552_F and DHL_P553_R. Primers DHL_P551_R and DHL_P552_F have the A206K[14] in the overhang. The PCR products were purified and inserted into the SacI/XmaI-digested pDHL19 vector with isothermal assembly[56].

pDHL970 was built by PCR amplifying the region corresponding to P_{clpPX}-*clpP*-mGFPmut3 from genomic DNA of strain DHL661 with primers DHL_P557_F and DHL_P558_R. The PCR product was cloned into pNDL1 with Gateway cloning (Invitrogen) and sequence-verified with primers M13_R, NL15_F and DHL_P184_F.

Primers

All primers and DNA oligonucleotides were purchased from Integrated DNA Technologies, Inc. (IDT) and are listed in **Supplementary Table 5**.

Fluorescent proteins

All fluorescent protein used in this study, including the SNAP tag, are listed in **Supplementary Table 1**.

Supplementary Methods 1

Western blot analysis

Overnight cultures of the respective *E. coli* strains were diluted 1:1,000 in LB medium and grown with shaking (220 rpm) at 37 ˚C until the cultures reached OD_{600} = 0.2–0.3. Then, 1,600 µl of cell suspension was pelleted (15,000 g, 1 min, room temperature), normalized by OD_{600} by resuspending the cell pellet in x µl (where x is $x = 160 \times OD_{600}$) of 1× SDS loading buffer (80 mM Tris-HCl pH 6.8, 2% (w/v) SDS, 10% (v/v) glycerol, 5% (w/v) ß-mercaptoethanol, 0.01% (w/v) bromphenol blue) and boiled at 95 ˚C for 5 min. 10 µl cell lysate per lane and 5 µl molecular weight marker (SeeBlue Plus2 Pre-Stained Standard, Invitrogen, cat# LC5925) were loaded on a 10% SDS page (Tris-glycine) and the proteins were separated. Next, the proteins were transferred to a 0.2 µm nitrocellulose membrane (Sigma-Aldrich, cat# N7892-5EA) by electroblotting (100 V, 1 h, 4 ˚C). After the transfer, the membrane was incubated in blocking buffer (1× TBS, 0.1% (v/v) Tween-20, 4% (w/v) milk powder) for 1 h at room temperature. Then, the membrane was incubated with a polyclonal rabbit anti-GFP antibody (courtesy of Prof. P. Silver, Harvard Medical School) for the Clp-FP fusions or polyclonal anti-SNAP tag antibody (NEB, cat# P9310S) for the Clp-SNAP tag fusions, diluted 1:1,000 in antibody dilution buffer (1× TBS, 2% (w/v) BSA, 0.1% (v/v) Tween-20, 0.05% (w/v) NaN_3), for overnight at 4 ˚C. The membrane was washed 4 times for 20 min in TBST (1× TBS, 0.1% (v/v) Tween-20) with gentle shaking. Next, the membrane was incubated with anti-rabbit HRP-linked secondary antibody (GE Healthcare, NA934V), diluted 1:5,000 in blocking buffer, for 1 h at room temperature. Lastly, the membrane was washed 4 times for 5 min with TBST and then the Western blot was developed with homemade ECL reagent.

Semi-quantitative Western blot analysis

Samples were prepared similarly to normal Western blot samples with the following modifications. Cells were diluted 1:2,000 and grown at 30 ˚C or 37 ˚C. 5 ml of exponentially growing cells (OD_{600} = 0.2–0.25) were harvested by centrifugation (3,200 g, 10 min, 4 ˚C), the supernatant was discarded and the cell pellet was frozen on dry ice for 15 min. Next, the pellet was resuspended in x µl (where x is $x = 100 \times OD_{600}$) of lysis buffer and incubated for 10 min on ice followed by a 10 min incubation at 37 ˚C on an inverter. The lysis buffer was prepared fresh before use and is composed of B-PER reagent (Thermo Scientific, prod# 78248) with 50 µg/ml lysozyme (Sigma-Aldrich, cat# L6876), Benzonase nuclease (Sigma-Aldrich, cat# E1014, used as a 2,000× stock) and 1× EDTA-free protease inhibitor cocktail (Roche, cat# 11 873 580 001, 1 tablet dissolved in 2 ml H_2O was used as a 25× stock). The total protein concentration of the cell lysate was determined with the Bio-Rad DC Protein Assay (Bio-Rad, cat# 500-0116) according to the manufacturer's instruction manual. The samples were diluted with H_2O and 4× SDS loading buffer to 1× final, boiled for 5 min at 95 ˚C and 10 or 25 µg of total cell lysate was loaded per lane. Transfer, incubation and washing steps were carried out as previously described. The primary antibodies used were polyclonal rabbit anti-ClpX (described below) and anti-ClpP antibodies (lab collection of Prof. T. Baker, MIT) and were diluted 1:3,000 and 1:5,000 respectively in antibody dilution buffer. After visualization of the ClpX and ClpP bands, the membranes were washed twice for 20 min

in 1× TBST, blocked again and re-probed with a mouse monoclonal anti-Sigma70 antibody (Neoclone, cat# WP004) to measure the sigma70 (also known as RpoD) levels as a loading control. The primary anti-Sigma70 antibody was diluted 1:1,000 in antibody dilution buffer and the anti-mouse HRP-linked secondary antibody (GE Healthcare, NA931V) was diluted 1:5,000 in blocking buffer. The Western blot was developed with homemade ECL reagent.

SUPPLEMENTARY REFERENCES

20. Wong, W.W., Tsai, T.Y. & Liao, J.C. *Mol. Syst. Biol.* **3**, 130 (2007).
21. Tsien, R.Y. *Annu. Rev. Biochem.* **67**, 509-544 (1998).
22. Maurizi, M.R. *et al*. *J. Biol. Chem.* **265**, 12536-12545 (1990).
23. Azam, T.A., Hiraga, S. & Ishihama, A. *Genes Cells* **5**, 613-626 (2000).
24. Diestra, E., Cayrol, B., Arluison, V. & Risco, C. *PLoS One* **4**, e8301 (2009).
25. Subach, O.M. *et al. Chem. Biol.* **15**, 1116-1124 (2008).
26. Chudakov, D.M., Lukyanov, S. & Lukyanov, K.A. *Nat. Protoc.* **2**, 2024-2032 (2007).
27. Pedelacq, J.D., Cabantous, S., Tran, T., Terwilliger, T.C. & Waldo, G.S. *Nat. Biotechnol.* **24**, 79-88 (2006).
28. Lawrence, M.S., Phillips, K.J. & Liu, D.R. *J. Am. Chem. Soc.* **129**, 10110-10112 (2007).
29. Ando, R., Mizuno, H. & Miyawaki, A. *Science* **306**, 1370-1373 (2004).
30. Stiel, A.C. *et al. Biochem. J.* **402**, 35-42 (2007).
31. McKinney, S.A., Murphy, C.S., Hazelwood, K.L., Davidson, M.W. & Looger, L.L. *Nat. Methods* **6**, 131-133 (2009).
32. Gurskaya, N.G. *et al. Nat. Biotechnol.* **24**, 461-465 (2006).
33. Griesbeck, O., Baird, G.S., Campbell, R.E., Zacharias, D.A. & Tsien, R.Y. *J. Biol. Chem.* **276**, 29188-29194 (2001).
34. Heikal, A.A., Hess, S.T., Baird, G.S., Tsien, R.Y. & Webb, W.W. *Proc. Natl. Acad. Sci. USA* **97**, 11996-12001 (2000).
35. Nagai, T. *et al. Nat. Biotechnol.* **20**, 87-90 (2002).
36. Elf, J., Li, G.W. & Xie, X.S. *Science* **316**, 1191-1194 (2007).
37. Nguyen, A.W. & Daugherty, P.S. *Nat. Biotechnol.* **23**, 355-360 (2005).
38. Reyes-Lamothe, R., Sherratt, D.J. & Leake, M.C. *Science* **328**, 498-501 (2010).
39. Shaner, N.C. *et al. Nat. Methods* **5**, 545-551 (2008).
40. Shcherbo, D. *et al. Biochem. J.* **418**, 567-574 (2009).
41. Shaner, N.C. *et al. Nat. Biotechnol.* **22**, 1567-1572 (2004).
42. Sauter, C., Basquin, J. & Suck, D. *Nucleic. Acids. Res.* **31**, 4091-4098 (2003).
43. Yoshimoto, T., Murayama, N., Honda, T., Tone, H. & Tsuru, D. *J. Biochem.* **104**, 93-97 (1988).
44. Wilce, M.C. *et al. Proc. Natl. Acad. Sci. USA* **95**, 3472-3477 (1998).
45. Kitagawa, M., Miyakawa, M., Matsumura, Y. & Tsuchido, T. *Eur. J. Biochem.* **269**, 2907-2917 (2002).
46. Ratajczak, E. *et al. FEBS Lett.* **584**, 2253-2257 (2010).

47. Buschmeier B, H.W. & Deutscher J. *FEMS Microbiol. Lett.* **29**, 231-235 (1985).
48. Datsenko, K.A. & Wanner, B.L. *Proc. Natl. Acad. Sci. USA* **97**, 6640-6645 (2000).
49. McKenzie, G.J. & Craig, N.L. *BMC Microbiol.* **6**, 39 (2006).
50. Lutz, R. & Bujard, H. *Nucleic. Acids. Res.* **25**, 1203-1210 (1997).
51. Lanzer, M. & Bujard, H. *Proc. Natl. Acad. Sci. USA* **85**, 8973-8977 (1988).
52. Ajo-Franklin, C.M. *et al. Genes Dev.* **21**, 2271-2276 (2007).
53. Tu, G.F., Reid, G.E., Zhang, J.G., Moritz, R.L. & Simpson, R.J. *J. Biol. Chem.* **270**, 9322-9326 (1995).
54. Keiler, K.C., Waller, P.R. & Sauer, R.T. *Science* **271**, 990-993 (1996).
55. Cormack, B.P., Valdivia, R.H. & Falkow, S. *Gene* **173**, 33-38 (1996).
56. Gibson, D.G. *et al. Nat. Methods* **6**, 343-345 (2009).